Organic Electronics 15 (2014) 2847–2854

Contents lists available at ScienceDirect

Organic Electronics

journal homepage: www.elsevier.com/locate/orgel

Silver-loaded anatase nanotubes dispersed plasmonic composite photoanode for dye-sensitized solar cells

Hua Dong [a], Zhaoxin Wu [a,*], Yucui Gao [a], Ahmed El-Shafei [b], ShuYa Ning [a], Jun Xi [a], Bo Jiao [a], Xun Hou [a]

[a] Key Laboratory of Photonics Technology for information, Key Laboratory for Physical Electronics and Devices of the Ministry of Education, School of Electronic and Information Engineering, Xi'an Jiaotong University, Xi'an 710049, PR China
[b] Polymer and Color Chemistry Program, Textile Engineering, North Carolina State University, NC 27695, USA

ARTICLE INFO

Article history:
Received 12 May 2014
Received in revised form 5 August 2014
Accepted 7 August 2014
Available online 23 August 2014

Keywords:
Hybrid nanostructures
One-dimensional architecture
Surface plasmon resonance effect
Electron transport pathway
Dye-sensitized solar cells

ABSTRACT

In this article, a typical silver-loaded anatase TiO_2 nanotube (Ag-TNTs) was developed and assembled in DSSCs. By blending the Ag-TNTs and TiO_2 nanoparticles as the composite photoanode, this hybrid nanostructure exhibits a promising architecture for accelerating electron transport as well as enhancing dye adsorption. These nanotubes could provide direct charge transfer pathways and increase electrolyte penetration in comparison with the TiO_2 nanoparticles alone network. Moreover, the presence of the Ag nanoparticles could enhance the light harvesting efficiency and promote the charge separation, which further improves the performance of the DSSCs. The DSSC with metal-modified hybrid nanostructures has achieved an efficiency of 8.19% which is about 56% higher than DSSCs based on TiO_2 nanoparticles photoanode with 5.26%.

1. Introduction

In recent years, Dye-sensitized solar cells (DSSC) have attracted much attention and scientific research since 1991 [1]. With the advantages of being inexpensive, light weight, easy-fabrication and flexible, this type of solar cells has become available and considerable for reducing the cost of electricity generation [2]. Today, DSSCs has reached a power conversion efficiency as high as 12.3% [3]. A number of factors influence the performance of DSSCs. In particular, enhancing light-harvesting efficiency (LHE) and promoting the carrier transfer in film are the most desired factors to improve the performance of the DSSCs [4]. Developing one-dimensional (1D) architecture instead of random nanocrystalline structures as photoanode is a potential way for the better performance of DSSCs. Such as nanotubes, [5] nanowires [6] and other array structures, [7] can act as the single crystal and be beneficial of rapid electron transport. However, the major problems of 1D nanostructures are their poor adhesion with substrates, which leads to an insufficient surface area. Consequently, hybrid nanostructures, TiO_2 nanoparticles/1D nanostructures composite electrode have recently been expected as a more effective architecture for electron transport as well as dye adsorption [8,9]. The existence of the 1D structure is beneficial in electrolyte penetration and light scattering, and leads to the rapid electron transport in photoanode [10,11]. Also the hybrid structures without losing high surface area promise the enough absorbed dyes.

Besides the development of the hybrid nanostructure, surface plasmon resonance (SPR) of metal nanostructures has been regarded as another promising way to improve the performance of photovoltaic devices [12]. SPR effect is a light-induced collective oscillation of conduction band

* Corresponding author. Tel.: +86 29 82664867.
E-mail addresses: zhaoxinwu@mail.xjtu.edu.cn (Z. Wu), Ahmed_El-Shafei@ncsu.edu (A. El-Shafei).

http://dx.doi.org/10.1016/j.orgel.2014.08.020
1566-1199/

electrons on the surface of metal nanostructures [13]. A lot of related nanostructures have been designed and assembled in DSSCs to increase the light absorption and accelerate the charge separation. In this case, combining the hybrid architecture and SPR effect in DSSCs is expected to further improve the performance of photovoltaic devices by exploiting metal-modified hybrid photoanode.

Guided by this principle, we designed a kind of unique Ag-loaded titania nanotubes (Ag-TNTs) and prepared the Ag-TNTs/TiO_2 nanoparticles (NPs) composite photoanode in DSSCs. A dramatic increase in efficiency (8.19%) is achieved in device of Ag-TNTs/TiO_2 NPs in compared with that of TiO_2 NPs (5.26%). Our study shows that beyond the advantage of TNTs, the presence of Ag nanoparticles also delivers superior performance on photoelectric and photocatalytic properties. SPR effect stimulated by the Ag could enhance the light absorption of dye and the generation of the photoelectrons [14]. As to the electrical aspect, Ag nanoparticles could play a role as the electrons transport-separation center, which accelerated the electron to move through the photoanode network and reduced the charge recombination [15]. Furthermore, this type of photoanode can be fabricated by an ordinary paste coating technique. The high-efficiency, cost-effective and widely applicable electrodes have good prospects for developing the performance of the DSSCs.

2. Experiment details

2.1. Synthesis of Ag-loaded anatase TiO_2 nanotube

The anatase titanium dioxide nanotubes were prepared by the hydrothermal method [16]. Anatase titania powder 1 g and an aqueous solution of NaOH (50 ml, 10 M) were placed into the Teflon-lined autoclave. The mixture was kept stirred to form a colloidal suspension, then the mixture was sealed and hydrothermally treated at 160 °C for 20 h. The precipitate was separated by filtration and washed with deionized water until a pH value near 7 was reached. The precipitate was then ground in alcohol followed by ultrasonic-assisted dispersion and oven-dried at 60 °C until the sample was fully dried into powder. After that, the initial titanate nanotubes were obtained. The products were annealed at 600 °C for 2 h to crystallize into the anatase phase.

Ag-loaded TNTs were prepared as following: Adding a small amount NaOH to 20 ml ethylene glycol to adjust the PH of solution to 8; Adding 0.2 g anatase TNTs to the solution, then put the mixed solution under ultrasonic dispersion 30 min to form a colloidal suspension, adding 5 ml of the saturated solution of $AgNO_3$ (anhydrous ethanol as the solvent). Put the final mixed solution under magnetic stirring at 50 °C for 9 h, after cooled at room temperature, the mixed solution was centrifugal washing with anhydrous ethanol three times, then the precipitate was fully dried at 50 °C, at last we will get dark brown powder signed as the Ag-TNTs.

0.1 g original Ag-TNTs was added into 30 ml deionized water, then 0.02 g titanium tetraisopropoxide (TTIP) as the TiO_2 precursor was added in the solution, and stirring was continued for an additional 30 min at 60 °C to ensure completion of the reaction. Ag-TNTs with thin TiO_2 shell layer around the Ag nanoparticles were then obtained. The solution was washed several times and centrifuged at 3000 rpm to remove TTIP.

2.2. Fabrication of photoanodes and DSSCs

Glass substrates coated FTO (Nippon Sheet Glass, Japan, 2.2 mm thickness, 14 $\Omega\,\square^{-1}$) were cleaned in a detergent solution for 30 min in an ultrasonic bath, rinsed with deionized water, isopropanol and ethanol for 30 min successively. The pure TiO_2 pastes were prepared by TiO_2 powder (Degussa, P25), devices with different photoanodes were synthesized by stirring various pure nanotubes and Ag-loaded nanotubes and into the TiO_2 pastes according to a series of mass ratios (TiO_2 NPs = 100%; TNTs = 5%, 10%, 20%, 30%, 50%, 100%; Ag-TNTs = 5%, 10%, 20%, 30%). Then these kinds of transparent TiO_2 pastes were screen-printed onto the FTO as the transparent layer, then the coated films were dried at temperature of 125 °C for 6 min. This screen-printing procedure with the paste was repeated to obtain an appropriate thickness of 8 μm of TiO_2 for the working electrode. The coated substrates were thermally treated under an air flow at 325 °C for 5 min, 375 °C for 10 min, 450 °C for 15 min and 500 °C for 15 min, respectively. After cooling down to 80 °C, the TiO_2 electrode was stained by immersing it into a dye solution containing N719 sensitizer (300 μM) in a mixture of acetonitrile and tert-butyl alcohol (volume ratio: 1:1) overnight. The TiO_2 photoanodes absorbed dye and 2 nm Pt counter electrodes were assembled into a sealed sandwich-type cell by a 60 μm hot-melt ionomer film Bynel (DuPont) as a spacer between the electrodes. A drop of the electrolyte solution, 0.6 M 1-butyl-3-methyl imidazolium iodide (BMII), 0.03 MI_2, 0.02 M LiI, 0.10 M guanidinium thiocyanate and 0.5 M 4-tert-butylpyridine in a mixture of acetonitrile and valeronitrile (volume ratio, 85:15), was injected into the cell.

2.3. Characterization

The morphology of the AgNW@TiO_2 was investigated by scanning electron microscopy (SEM) (Quanta 250, FEI) and transmission electron microscope (TEM) (2100, JEOL). The chemical species were analyzed by Energy-dispersive X-ray spectroscopy (EDX) (EDAX, Quanta 250, FEI). The crystalline structure of the various TiO_2 films was determined by X-ray diffraction (XRD) (D/MAX-2400, Rigaku, Japan). The UV–Vis absorption spectra were obtained on a UV–Vis spectrophotometer (Fluoromax 4, HORIBA Jobin Yvon, USA). The Incident Photon-to-current Conversion Efficiency (IPCE) was evaluated by the solar cell quantum efficiency measurement system (SolarCellScan 100, Zolix instruments. Co. Ltd). The photocurrent density-voltage characteristics were evaluated by an AAA solar simulator (XES-301S, SAN-EI Electric. Co. Ltd.), AM 1.5G illumination (100 mW cm^{-2} in intensity), and a Keithley digital source meter (Model 2602). Electrochemical impedance spectra (EIS) of the cells were evaluated using CHI-660D over the frequency range of 1 Hz ~ 100 KHz under the conditions

of different bias-voltage. All the cells have an active area about 0.25 cm^2.

3. Result and discussion

3.1. Properties of the nanotubes

The initial titanate TNTs were obtained via the hydrothermal method. The SEM image (Fig. 1a and b) and TEM image (Fig. 1d) of the as-synthesized TNTs show that these TNTs are hundreds of nanometers in length with a uniform diameter (~10 nm) and high aspect ratio. To obtain the effective hybrid matrix, doped TiO_2 TNTs should preferably have the same crystal structure as nanoparticles for effective electron transport [4]. The mechanical strength should also be reinforced. And the mechanical strength should also be reinforced. As a consequence, A high-temperature treatment was essential. After annealing the titanate TNTs at 600 °C, the anatase products are prepared. Fig. 1c shows the SEM image of the annealed nanostructures. It can be seen that part of the nanotubes formed the nanorods and nanoribbons, and uniformity is slightly degenerate. However, most of the nanostructures still remain the 1-D architecture, which could provide the electron transfer pathway and improve the electron transfer ability for the better performance of DSSCs.

Fig. 1(e) and (f) shows the TEM images of the Ag-TNTs. Ag nanoparticles were well dispersed on the external surface of anatase TNTs by chemical deposition method. It was noted that the chemical and thermal stability of the plasmonic nanostructure was the premise of the application in DSSCs, so the treatment process of the Ag-TNTs for forming a protecting layer was needed. In our experiments, hydrolysis of titanium precursors was used to deal with the original Ag-TNTs, and then the thin TiO_2 shell around the Ag nanoparticles was formed to avoid corrosion and deformation. The diameter of Ag nanoparticles embedded in the TNTs is nearly 5 nm. The EDX spectrum is used to analyze the ingredient of the Ag-TNTs and the result is shown in Fig. S1†. The rough percentage concentrations by weight of Ti and Ag were estimated about 32.27% and 8.53%, respectively (shown in Table S1†). From the XRD patterns of the TNTs and Ag-TNTs which are shown in Fig. 2a, the as-synthesized TNTs annealed at 600 °C exhibit the anatase phase. Additionally, diffraction peaks of Ag (1 1 1) were also found in the patterns of the Ag-TNTs, indicating the presence of the Ag nanoparticles. UV–Vis absorption spectrum of the treated Ag-TNTs was shown in Fig. 2b. It was found that the Ag-TNTs display the wide absorption spectrum in the visible region, and the resonance peak of Ag at 439 nm could be observed clearly. The strong absorption in the visible region of the Ag-TNTs could provide the superior photocatalytic performance, and the SPR effect of Ag can be effectively stimulated to enhance the light-harvesting efficiency of the photoanode.

To confirm the stability of the treated Ag-TNTs, UV–Vis absorption spectrum of the bare and treated Ag-TNTs in electrolyte were shown in Fig. S2a† and b†. In Fig. S2a†, the absorption peak Ag NPs disappear after mixed with electrolyte after a period of time, which is due to the corrosion of iodide/triiodide redox couple. However, the absorption property of treated Ag-TNTs shown in Fig. S2b† has almost unchanged. The comparison indicated that the application of treated Ag-TNTs with excellent chemical stability in DSSCs was realizable.

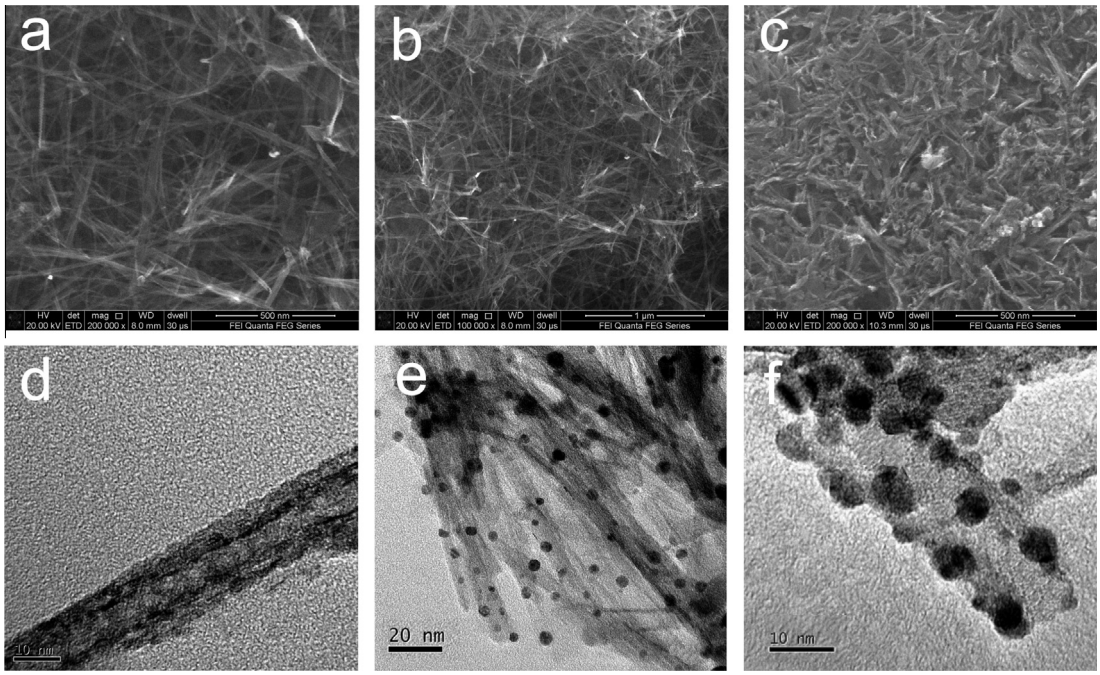

Fig. 1. (a and b) SEM images and (d) TEM image of the initial TNTs; (c) SEM image of the anatase TNTs and (e and f) TEM images of the Ag-TNTs.

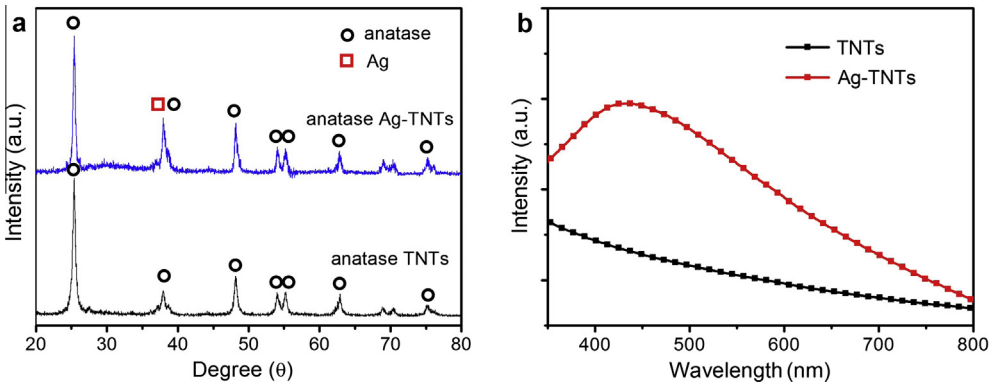

Fig. 2. (a) X-ray diffraction (XRD) patterns of TNTs and Ag-TNTs and (b) Absorption spectrum of the different materials in ethanol.

Ahead of the preparation of the Ag-TNTs incorporated DSSCs, firstly we have assembled DSSCs with various concentration of anatase TNTs added to TiO_2 nanoparticles for photoanodes (0%, 5%, 10%, 20%, 30%, 50%, 100%), and the best performance is obtained at 10%. (shown in Fig. S3†.) To illustrate the superiority of the Ag-TNTs compared with the pure TNTs, the final research system is designed as TiO_2 NPs, TNTs/TiO_2 NPs (10%:90%) and Ag-TNTs/TiO_2 NPs (5%:95%, 10%:90%, 20%:80% and 30%:70%). Meanwhile, the ratio of Ag-TNTs in photoanodes was also optimized to further improve the efficiency. The reason is that insufficient amounts of silver could not effectively enhance the light harvesting efficiency and excess amounts could lead to the low surface area of photoanode.

3.2. Absorption and FDTD simulation

In our experiment, the schematic structures are three types of devices with different photoanodes (TiO_2 NPs, TNTs/TiO_2 NPs and Ag-TNTs/TiO_2 NPs), and the schematic was shown in Fig. 3. In compared with the TiO_2 NPs and TNTs/TiO_2 NPs structure, the Ag-TNTs/TiO_2 NPs with the SPR effect exhibits the unique capability in enhancing the light harvesting efficiency. In order to evaluate the contributions of the Ag-TNTs on the light-harvesting effect, the absorption spectrums of the dye-absence/adsorbed/desorbed photoanode films were measured and shown in Fig. 4. Fig. 4a shows the absorption spectrums of the dye-absence films. It can be seen that SPR band is observed in different films with Ag-TNTs, which indicated that the thermostability of the treated Ag NPs is acceptable. This is also the premise of the Ag-TNTs applied in the DSSCs.

Referring to the TiO_2 NPs and TNTs/TiO_2 NPs, from the adsorption/desorption spectrum, it was found that the amount of dyes adsorbed on TNTs/TiO_2 NPs film is slightly less than that of TiO_2 NPs film, whereas the adsorption intensity of dye-absorbed films has the opposite tendency that the TNTs/TiO_2 NPs is slightly stronger. This meaningful phenomenon is attributed to the light scattering ability of the TNTs, which reveals an advantage of the TNTs for the higher performance of DSSCs [6].

When discussing the Ag-TNTs/TiO_2 NPs film, the absorption intensity of the Ag-TNTs/TiO_2 NPs films increased with the Ag-TNTs increased, enhancing remarkably compared to the other two films. Whereas the desorbed adsorption intensity of films with Ag-TNTs is slightly lower than the pure TiO_2 film, indicating that the amount of loaded dye is less. These results demonstrated that besides the light scattering effect of the TNTs, the enhanced absorption of the Ag-TNTs/TiO_2 NPs photoanode is mainly attributed from

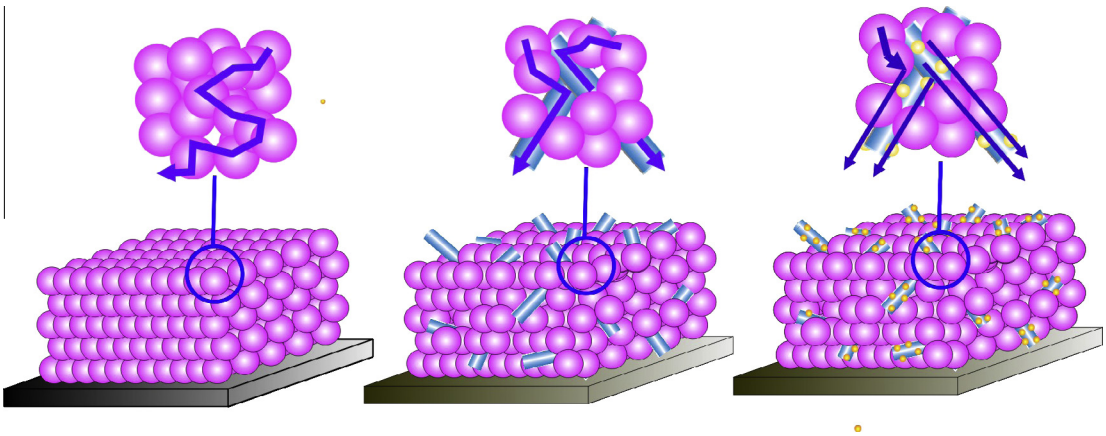

Fig. 3. Schematic structure of three kinds of photoanodes.

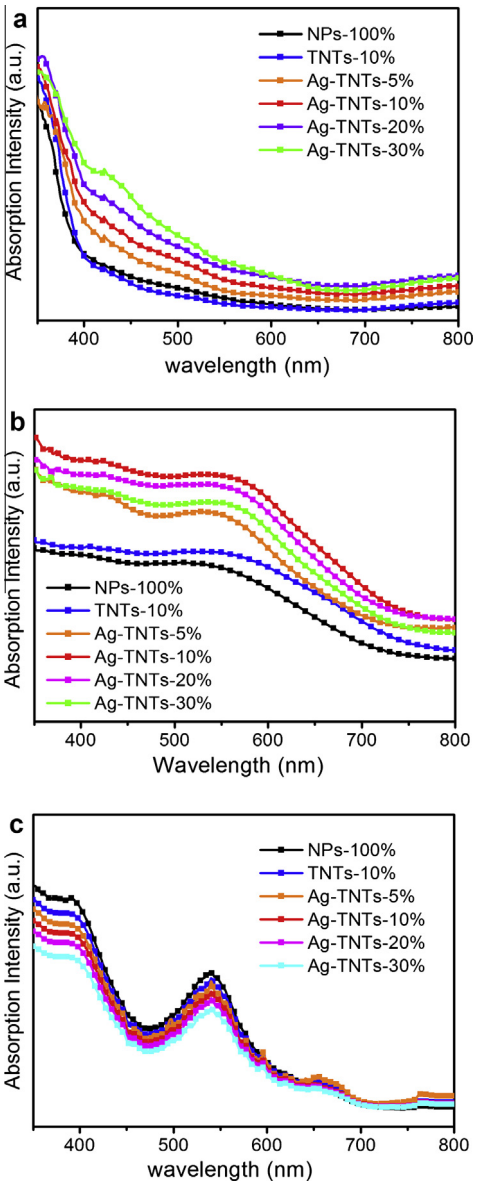

Fig. 4. (a) Absorption spectrum of the different TiO_2 photoanodes without dyes. (b) Absorption spectrum of the different TiO_2 photoanodes absorbed dyes. (c) Absorption spectra of the desorbed N719 from dye-loaded TiO_2 film in NaOH solution.

the SPR effect and light scatter effect of Ag nanoparticles [17]. SPR effect of the composite stimulated by illumination light leads to the collective excitation oscillations and thus created a strong enhancement of the localized electromagnetic fields around the Ag nanoparticles. By the enhanced electromagnetic field improving the interaction with the dye molecule dipoles, the enhanced light absorption of the dye and more charge carrier generation can be achieved [18]. In addition, the light-scattering property of the resonant Ag nanoparticles provided extra optical pathways for the superior performance.

It is noted that as the concentration of Ag-TNTs increased, the absorption intensity of the films have almost no obvious increasement. Meanwhile, it can be seen films with higher concentration of Ag-TNTs adsorbed less dyes (shown in Fig. 4b). This phenomenon indicated that only appropriate Ag-TNTs ratio of the photoanode could maintain a balance between the effective SPP effect and enough amounts of absorbed dyes. To further clarify the plasmonic behaviors of the Ag-TNTs, theoretical investigation on spatial properties of light trapping by plasmonic effect is developed. Finite Difference Time Domain method (FDTD) is applied to calculate the electric field intensity distributions and the result is shown in Fig. 5 (Lumerical FDTD solutions). The geometry of a single Ag-TNT is modeled as a cylinder in the air with Ag nanoparticles loaded, and the density of Ag NPs in the model was kept similar as synthetic structure. An incident planewave at $\lambda_0 = 450$ nm stimulated the structure to obtain the LSPR effect. It was found that local field intensity surround the Ag-TNTs is strongly enhanced, and the enhanced local field almost covered the whole space around the TNT. This result indicated that a sparse distribution of Ag NPs could promise the achievement of the SPR effect which fully promoted the absorption of the photoanode. So photoanodes with suitable concentration of Ag-TNTs could achieve effective SPR effect as well as adsorb enough amounts of dyes. This unique characteristic is beneficial to boost the J_{sc} and the power conversion efficiency of DSSCs.

3.3. I–V and IPCE characteristics

To investigate the impact of optics-electrics properties of Ag-TNTs on the performance of DSSCs, the current–voltage (I–V) and incident photon-to-current conversion efficiency (IPCE) characteristics of DSSCs with various photoanodes were discussed in this section. To demonstrate the advantages of Ag-TNTs on DSSCs, a series ratios of devices with TNTs/TiO_2 NPs photoanodes were studies firstly (Fig. S3†). Results show that 10% TNTs exhibites the best performance. So referring to the focal research system in our experiment, DSSCs with series of photoanodes (100% TiO_2 NPs, 10% TNTs, 5% Ag-TNTs, 10% Ag-TNTs, 20% Ag-TNTs and 30% Ag-TNTs) were designed and studied.

Fig. 6 shows the *I–V* amd IPCE curves of devices. To compare with the pure TiO_2 NPs, the short-circuit current density (J_{sc}) and the power conversion efficiency (η) were significantly modified with the introduction of TNTs and Ag-TNTs (results displayed in Table 1). Since the values of the fill factor (FF) and V_{oc} remain nearly constant, the enhancement of the J_{sc} is the reason of the improvement the power efficiency. About the device with TNTs 10 wt%, the significant enhancement of the J_{sc} superior to the TiO_2 NPs alone is due to the capability of the electron transport pathway provided by the TNTs. Moreover, the introduction of anatase TNTs to the TiO_2 NPs (P25, anatase phase: rutile phase$\sim$7:3) increased the ratio of the anatase, which improves the photovoltaic characteristic [19].

For the device with Ag-TNTs/TiO_2 NPs, a increasing-decreasing trend of the power efficiency of the DSSCs can be observed. The optimized and further dramatic enhanced efficiency of devices is obtained at 10 wt% compared to that with TNTs at the same concentration. This remarkable

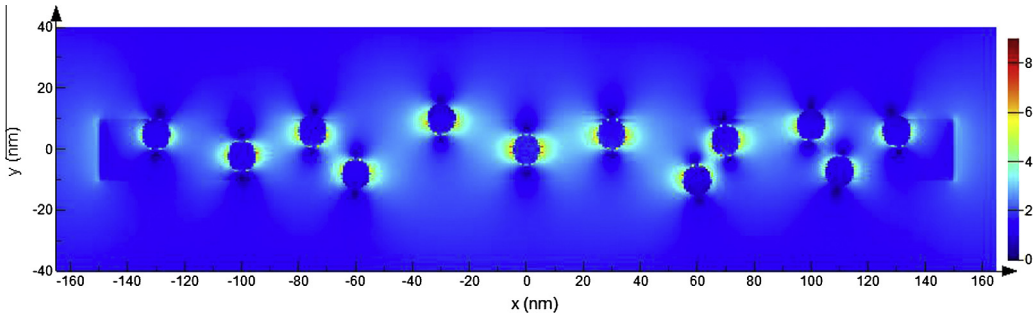

Fig. 5. The calculated distribution of electric field amplitude intensity around Ag-TNTs.

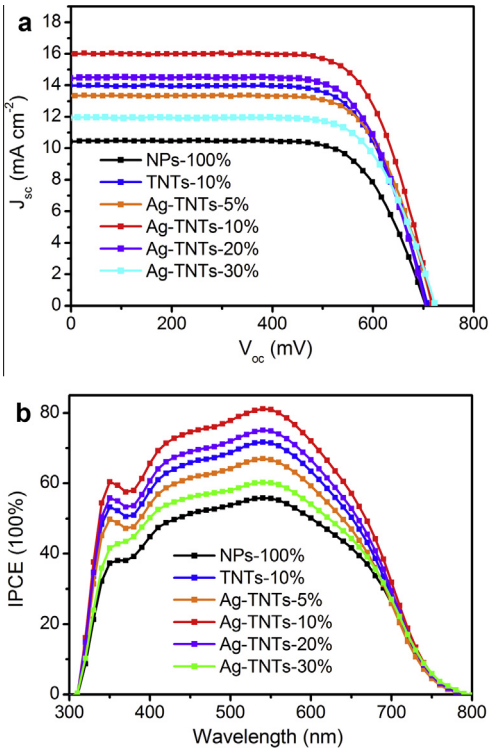

Fig. 6. (a) *I–V* and (b) IPCE characteristic of DSSCs with various TiO_2 photoanodes.

Table 1
Photovoltaic characteristics of DSSCs.

Devices	V_{oc} (mV)	J_{sc} (mA cm^{-2})	FF	η (%)	R_{ct} (Ω)
Pure TiO_2 NPs	705	10.43	0.710	5.26	37.47
10% TNTs	711	13.99	0.703	6.98	69.16
5% Ag-TNTs	718	13.34	0.712	6.83	51.87
10% Ag-TNTs	716	16.01	0.711	8.19	78.99
20% Ag-TNTs	708	14.45	0.706	7.29	57.74
30% Ag-TNTs	719	11.95	0.709	6.14	48.92

enhancement can be attributed to the following reasons. On one hand, the presence of TNTs could accelerate the electron transfer and suppress the recombination, and the interpenetration property of electrolyte in the hybrid matrix is also improved [11]. On the other hand, the SPR effect of Ag NPs is beneficial to improve the light harvesting efficiency, and the schottky barrier at the Ag/TiO_2 interface will form electron-hole separation centers for improving the movement of photo-generated electrons transporting from excited dye to TiO_2 nanoparticles, and thus the recombination of carriers is reduced [20]. To confirm the capability of charge separation by Ag nanoparticles attached on TNTs, the PL spectra of different films are shown in Fig. 7. PL spectra are often used to study the surface processes involving electron–hole recombination of semiconductors [23]. The broad-band emission around 410 nm (excited at 325 nm) can be assigned to the recombination of photoexcited holes with electrons occupying the singly ionized oxygen vacancies in TiO_2. The PL intensity in Ag-TNTs largely reduced compared to Ag-absence TNTs indicates that the recombination of electron–hole pairs has been suppressed deeply.

It is note that J_{sc} and η of the DSSCs decrease when the concentration is over 10 wt%. Considering that the absorption intensity of dye-adsorbed films in these DSSCs ($\geqslant$10%) is almost no difference, the decreased parameters can be attributed to less amounts of dyes and the negative charge recombination. That is, excess amount of Ag-TNTs may cluster to form larger Ag-NP groups and destroy the throughness of the TiO_2 network. The tendency of IPCE is consistent with the J_{sc}, which indicated that the

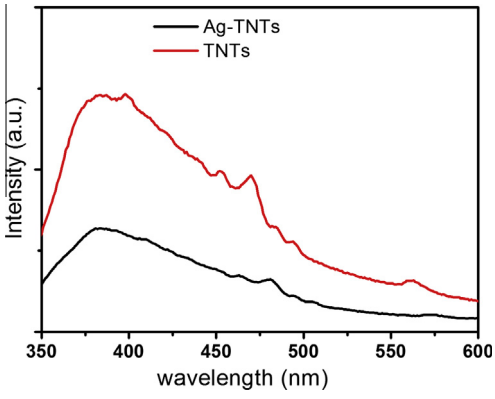

Fig. 7. Photoluminescence (PL) spectra of TNTs and Ag-TNTs.

introduction of the Ag-TNTs improves the light harvesting efficiency and the charge transport properties of the DSSCs.

3.4. EIS measurement and photocatalysis analysis

Electrochemical impedance spectroscopy is introduced as a useful technique to reveal the electrons transport-recombination processes in different DSSCs. The Nyquist plots of the obtained EIS data are shown in Fig. 8a (dark condition, −700 mV bias-voltage). From left to the right, the first semicircle portion (high frequency) in the Nyquist plots corresponds to the reduction reaction at the counter electrode, and the second semicircle is assigned to charge transfer at the TiO_2/dye/electrolyte interface. With the established physical models and equivalent circuits, the kinetics of electrical transport and recombination can be considered in terms of a combination of resistance and capacitors [21]. Due to the fact that our study focused on the photoanodes, the charge-transfer resistance $R_{ct,}$ relating to the recombination of electrons at the TiO_2/dye/electrolyte interface was mainly discussed and shown in Table 1.

Compared to the device with TiO_2 NPs only, R_{ct} values of the device with TNTs and Ag-TNTs are larger. The result shows that the introduction of TNTs and Ag-TNTs could suppress the charge recombination due to their different capability, and the schematic of electrons dynamics process was shown in Fig. 3. The devices contain TNTs could provide the transport pathway for the electrons and reduce the electron scattering, which lead to rapid electron transfer. Device with Ag-TNTs/NPs exhibits a more superior performance for its dual nature. In addition to the effect of TNTs for reducing the recombination, Ag-NPs acts as electron-hole separation centers as Schottky barriers at the Ag/TiO_2 interface successfully reduce charge recombination reaction between electrons emanating from TiO_2 films and redox couples present in the electrolyte [22]. It is found that the Rct of device with 10 wt% Ag-TNTs has the maximum value and then decrease with the concentration increased, which indicated that excess Ag-TNTs has the weak suppression of the charge recombination.

Electron lifetime can provide further information on the electron transport-recombination in DSSCs [24]. Fig. 8b shows the electron lifetime (τ) of different devices derived from the EIS measurements. Compared to the devices with TiO_2 NPs only, devices with TNTs exhibit a longer electron lifetime which suggested the addition of TNTs significantly increases the electron transport pathway, the electrolyte penetration and then reduces recombination. The longest lifetime was obtained at devices with Ag-TNTs at 10 wt%, and it reflected the superior capability of reducing recombination compared with the device with TNTs at the same concentration. The trend of life time is consistent with the R_{ct} and power efficiency, which embodied the contributions of the Ag-TNTs on the electrical property of the DSSCs.

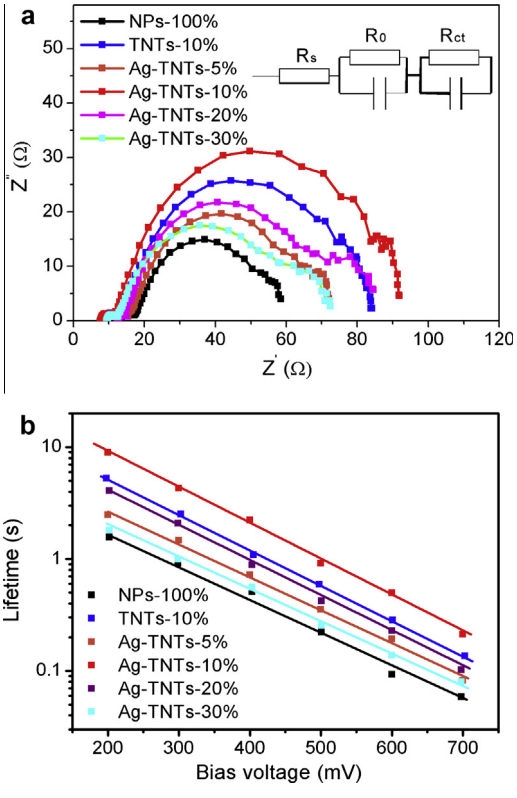

Fig. 8. Electrochemical impedance spectra (a) and lifetime (b) of DSSCs.

4. Conclusion

A typical Ag-loaded anatase TiO_2 nanotube was prepared and used as composite photoanodes for DSSCs via an easy-fabrication process. The metal-modified hybrid photoanode shows a significantly enhanced photovoltaic performance compared to those prepared from TiO_2 nanoparticles or nanotubes. Light harvesting efficiency can be improved via the SPR effect by the Ag nanoparticles. Moreover, efficient electron transport pathway and faster charge-separation can be achieved which suppress the recombination of electrons in the conduction band of TiO_2 with triiodide. The optimal properties were obtained in the device with Ag-TNTs/TiO_2 NPs photoanode, and the photoelectric conversion efficiency of the device with typical photoanode (8.19%) is greatly superior to those of DSSCs using pure TiO_2 photoanodes (5.26%).

Acknowledgements

This work was financially supported by Basic Research Program of China (2013CB328705), National Natural Science Foundation of China (Grant Nos. 61275034, 61106123), Ph.D. Programs Foundation of Ministry of Education of China (Grant No. 20130201110065); Fundamental Research Funds for the Central Universities (Grant No. xjj2012087); The SEM and TEM work was done at International Center for Dielectric Research (ICDR), Xi'an Jiaotong University, Xi'an, China; The authors also thank Ms. Dai for her help in using SEM and TEM.

Appendix A. Supplementary material

Supplementary data associated with this article can be found, in the online version, at http://dx.doi.org/10.1016/j.orgel.2014.08.020.

References

[1] B. Oregan, M. Gratzel, A low-cost, high-efficiency solar-cell based on dye-sensitized colloidal TiO_2 films, Nature 353 (1991) 737–740.

[2] S. Ito, T.N. Murakami, P. Comte, P. Liska, C. Gratzel, M.K. Nazeeruddin, M. Gratzel, Fabrication of thin film dye sensitized solar cells with solar to electric power conversion efficiency over 10%, Thin Solid Films 516 (2008) 4613–4619.

[3] A. Yella, H.W. Lee, H.N. Tsao, C.Y. Yi, A.K. Chandiran, M.K. Nazeeruddin, E.W.G. Diau, C.Y. Yeh, S.M. Zakeeruddin, M. Gratzel, Porphyrin-sensitized solar cells with cobalt (II/III)-based redox electrolyte exceed 12 percent efficiency, Science 334 (2011) 629–634.

[4] V. Thavasi, V. Renugopalakrishnan, R. Jose, S. Ramakrishna, Controlled electron injection and transport at materials interfaces in dye sensitized solar cells, Mater. Sci. Eng. R 63 (2009) 81–99.

[5] G.K. Mor, K. Shankar, M. Paulose, O.K. Varghese, C.A. Grimes, Use of highly-ordered TiO_2 nanotube arrays in dye-sensitized solar cells, Nano Lett. 6 (2006) 215–218.

[6] M. Durr, A. Schmid, M. Obermaier, S. Rosselli, A. Yasuda, G. Nelles, Low-temperature fabrication of dye-sensitized solar cells by transfer of composite porous layers, Nat. Mater. 4 (2005) 607–611.

[7] M.Y. Song, Y.R. Ahn, S.M. Jo, D.Y. Kim, J.P. Ahn, TiO_2 single-crystalline nanorod electrode for quasi-solid-state dye-sensitized solar cells, Appl. Phys. Lett. 87 (2005).

[8] K. Fujihara, A. Kumar, R. Jose, S. Ramakrishna, S. Uchida, Spray deposition of electrospun TiO_2 nanorods for dye-sensitized solar cell, Nanotechnology 18 (2007).

[9] Y. Suzuki, S. Ngamsinlapasathian, R. Yoshida, S. Yoshikawa, Partially nanowire-structured TiO_2 electrode for dye-sensitized solar cells, Cent. Euro. J. Chem. 4 (2006) 476–488.

[10] C.H. Ku, J.J. Wu, Electron transport properties in ZnO nanowire array/nanoparticle composite dye-sensitized solar cells, Appl. Phys. Lett. 91 (2007).

[11] S. Pavasupree, S. Ngamsinlapasathian, M. Nakajima, Y. Suzuki, S. Yoshikawa, Synthesis, characterization, photocatalytic activity and dye-sensitized solar cell performance of nanorods/nanoparticles TiO_2 with mesoporous structure, J. Photochem. Photobiol. A 184 (2006) 163–169.

[12] A. Takai, P.V. Kamat, Capture, store, and discharge. Shuttling photogenerated electrons across TiO_2-silver interface, Acs Nano 5 (2011) 7369–7376.

[13] J.R. Lakowicz, K. Ray, M. Chowdhury, H. Szmacinski, Y. Fu, J. Zhang, K. Nowaczyk, Plasmon-controlled fluorescence: a new paradigm in fluorescence spectroscopy, Analyst 133 (2008) 1308–1346.

[14] M.D. Brown, T. Suteewong, R.S.S. Kumar, V. D'Innocenzo, A. Petrozza, M.M. Lee, U. Wiesner, H.J. Snaith, Plasmonic dye-sensitized solar cells using core–shell metal–insulator nanoparticles, Nano Lett. 11 (2011) 438–445.

[15] J.F. Qi, X.N. Dang, P.T. Hammond, A.M. Belcher, Highly efficient plasmon-enhanced dye-sensitized solar cells through metal@oxide core–shell nanostructure, Acs Nano 5 (2011) 7108–7116.

[16] X.M. Sun, Y.D. Li, Synthesis and characterization of ion-exchangeable titanate nanotubes, Chem-Eur. J. 9 (2003) 2229–2238.

[17] Z.B. Tian, L.Q. Wang, L.S. Jia, Q.B. Li, Q.Q. Song, S. Su, H. Yang, A novel biomass coated Ag-TiO_2 composite as a photoanode for enhanced photocurrent in dye-sensitized solar cells, Rsc Adv. 3 (2013) 6369–6376.

[18] Y.Y. Lou, S. Yuan, Y. Zhao, P.F. Hu, Z.Y. Wang, M.H. Zhang, L.Y. Shi, D.D. Li, Molecular-scale interface engineering of metal nanoparticles for plasmon-enhanced dye sensitized solar cells, Dalton Trans. 42 (2013) 5330–5337.

[19] H. Lee, J.I. Park, T.H. Kim, K.B. Park, Efficiency of dye-sensitized solar cells based on TiO_2 nanoparticle/nanowire composites, J. Cera. Process. Res. 14 (2013) 405–409.

[20] K.M. Guo, M.Y. Li, X.L. Fang, X.L. Liu, B. Sebo, Y.D. Zhu, Z.Q. Hu, X.Z. Zhao, Preparation and enhanced properties of dye-sensitized solar cells by surface plasmon resonance of Ag nanoparticles in nanocomposite photoanode, J. Power Sources 230 (2013) 155–160.

[21] L.Y. Han, N. Koide, Y. Chiba, T. Mitate, Modeling of an equivalent circuit for dye-sensitized solar cells, Appl. Phys. Lett. 84 (2004) 2433–2435.

[22] J.M. Herrmann, J. Disdier, P. Pichat, Photoassisted platinum deposition on TIO_2 powder using various platinum complexes, J. Phys. Chem. 90 (1986) 6028–6034.

[23] M.D. Ye, D.J. Zheng, M.Q. Lv, C. Chen, C.J. Lin, Z.Q. Lin, Hierarchically structured nanotubes for highly efficient dye-sensitized solar cells, Adv. Mater. 25 (2013) 3039–3044.

[24] Z.Z. Yang, T. Xu, S.M. Gao, U. Welp, W.K. Kwok, Enhanced electron collection in TiO_2 nanoparticle-based dye-sensitized solar cells by an array of metal micropillars on a planar fluorinated tin oxide anode, J. Phys. Chem. C 114 (2010) 19151–19156.